Diode laser spectroscopy of carbon dioxide at 780 nm and methane at 840 nm

A. Lucchesini, S. Gozzini

IPCF – CNR - Area della Ricerca di Pisa

E-mail: lucchesini@ipcf.cnr.it

Introduction

Commercially available diode lasers DLs are suitable sources for high resolution spectroscopy of many molecules like CH_4, C_2H_2, C_2H_4, CHF_3, CO, CO_2, H_2O, H_2S, HCl, HCN, HF, NH_3, NO, NO_2, O_2, etc.. They can be modulated in order to use the noise reducting "frequency modulation" (FM) techniques.

Experimental set-up

The DL source is driven by a stabilized low-noise current supply. Its temperature is monitored by a high-stability thermal controller. The wavelength scan is obtained by adding a sawtooth signal to the driving current. The DL radiation goes through a confocal Fabry-Perot interferometer, through two Herriot type multipass cells (L= 30 m) containing the reference and the sample gases and also through a I_2 reference cell. A monochromator is used for a coarse wavelength measurement. For the harmonic detection a sinusoidal modulation current is mixed to the diode laser current: the transmitted signals are collected by silicon photodiodes and sent to a lock-in amplifier.

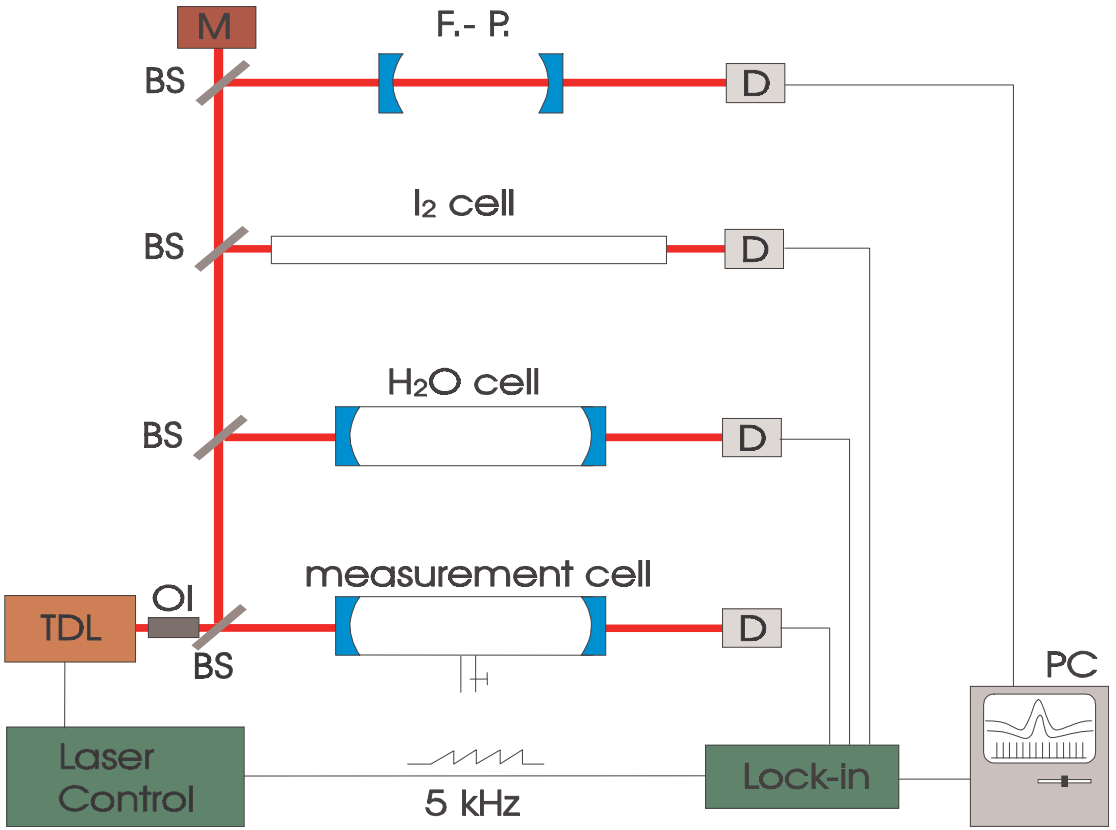

Fig. 1. Sketch of the experimental apparatus for the **FM** spectroscopy. **D**: photodiode; **OI**: optical insulator, **BS**: beam splitter; **F.-P.**: Fabry-Perot interferometer; **TDL**: tunable diode laser; **M**: monochromator; **PC**: desk-top computer.

Frequency modulation technique

When the DL emission radiation is modulated at the frequency $\nu_m = \omega_m/(2\pi)$ it can be described by $\nu = \bar{\nu} + a\cos\omega_m t$. If the DL emission is swept across the selected transition, the collected signal depends on both the line shape and the modulation parameters and can be written as a cosine Fourier series: $\tau(\bar{\nu} + a\cos\omega_m t) = \sum_{n=0}^{\infty} H_n(\bar{\nu}, a)\cos n\omega_m t$,

where H_n is the n-th harmonic component.

By demodulating the signal at a multiple $n\omega_m$ of the modulation frequency, an output signal proportional to the component H_n is collected, and if the amplitude a is chosen smaller than the width of the transition, the n-th Fourier component is proportional to the n-derivative of the original signal: $H_n(\bar{\nu}, a) = \frac{2^{1-n}}{n!} a^n \left.\frac{d^n \tau(\nu)}{d\nu^n}\right|_{\nu=\bar{\nu}}, \qquad n \geq 1$.

In particular we detected the second harmonic component (*2f* detection).

High modulation regime

In order to improve the signal to noise ratio (S/N) a large value of the modulation amplitude a is used, but this induces the derivative approximation to fail. Let's start form the general expression of the n-th harmonic component:

$H_n(x,m) = \epsilon_n\, i^n \int_{-\infty}^{+\infty} \hat{\tau}(\omega)\, J_n(m\omega)\, e^{i\omega x}\, d\omega$, where $\hat{\tau}(\omega) = \frac{1}{2\pi}\int \tau(x)\, e^{-i\omega x}\, dx$ is the Fourier transform of the transmittance profile; $x = \nu/\Gamma=$ and $m = a/\Gamma$ are respectively the frequency and the amplitude of the modulation, normalized to the line-width; J_n is the n-th order Bessel function; $\varepsilon_0 = 1$, $\varepsilon_n = 2$ ($n = 1, 2, ...$). The assumption of a Lorentzian absorption line-shape centered at $\nu = 0$ and half-width at half the maximum (HWHM) Γ_L is acceptable when the collisional broadening dominates, therefore the cross section coefficient will be $\sigma_L(x,m) \propto \frac{1}{1+(x+m\ cos\omega t)^2}$.

Following the works of Wahlquist and Arndt[1] we recalculated the second Fourier component of σ_L by putting $n = 2$:

$$H_2(x,m) = -\frac{1}{m^2}\left[\frac{\{[(1-ix)^2+m^2]^{\frac{1}{2}} - (1-ix)\}^2}{[(1-ix)^2+m^2]^{\frac{1}{2}}} + c.c.\right] .$$ Then, by eliminating the imaginary part:

$$H_2(x,m) = \frac{2}{m^2} - \frac{2^{\frac{1}{2}}}{m^2} \times \frac{\frac{1}{2}[(M^2+4x^2)^{\frac{1}{2}} + 1 - x^2][(M^2+4x^2)^{\frac{1}{2}} + M]^{\frac{1}{2}} + |x|\,[(M^2+4x^2)^{\frac{1}{2}} - M]^{\frac{1}{2}}}{(M^2+4x^2)^{\frac{1}{2}}}$$ with $M = 1 - x^2 + m^2$.

To obtain the line position parameters by the FM spectroscopy technique we fit the observed features by this function. The maximum S/N ratio has been obtained with the modulation index m = 2.2 – 2.3.

Experimental results

Carbon dioxide

An InGaAlAs SHARP Mod. LT025MD DL (λ = 785 nm, 40 mW cw) was adopted as the source. An example of spectrum is shown in **Fig. 2**, where six absorption resonances are near the R branch "turning point" at 782 nm.

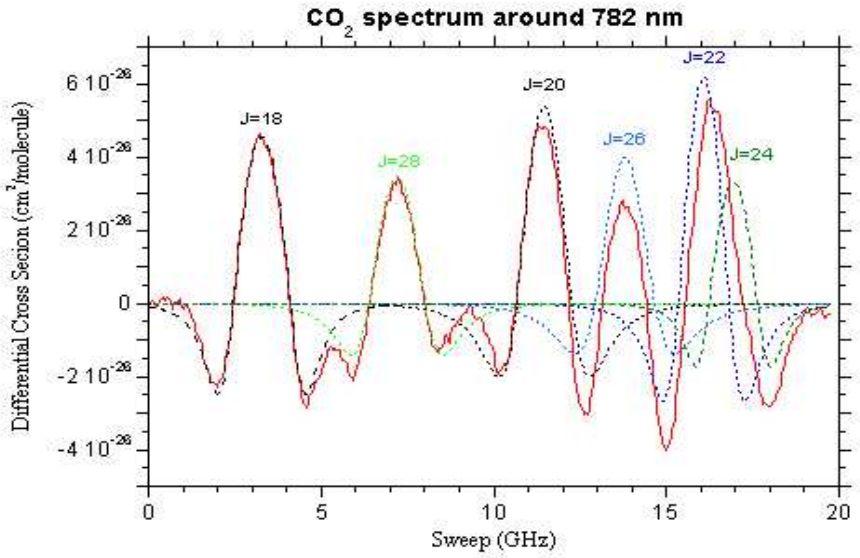

Fig. 2. 2nd derivative signal of the carbon dioxide transmission spectrum at ~ 782 nm obtained by FM spectroscopy, with 10 Hz bandwidth, p_{CO_2} = 91 Torr and room temperature. After the fit, the transitions are identified by their rotational quantum numbers.

The positions of the observed lines have been measured within 0.01 cm^{-1} with the aid of the I_2 reference cell and a precise absorption atlas[2]. **Table I** shows the results with the wavenumbers in vacuum. The corresponding wavelengths are in air at RT and have been deduced by using the index of refraction formula from the work of

Edlén[3]. The line positions correspond almost perfectly within the errors to the calculated ones by Campargue and colleagues[4].

Determination of the band parameters

To obtain the B_v, D_v rotational parameters and the ν_0 band origin we calculated the sums and combination differences of the measured line positions: $\Delta_2F''(J) = (4B'' - 6D'')\left(J+\frac{1}{2}\right) - 8D''\left(J+\frac{1}{2}\right)^3$, where $R(J-1) - P(J+1) = \Delta_2F''(J)$.

Usually $D''/B'' \approx 10^{-6}$, therefore: $\Delta_2F''(J) = 4B''\left(J+\frac{1}{2}\right) - 8D''\left(J+\frac{1}{2}\right)^3$.

From the linear regression fit shown in **Fig. 3** it comes out:

$$B_{000} = (0.39016 \pm 0.00005)\ \text{cm}^{-1} \quad \text{and} \quad D_{000} = (1.2 \pm 0.2)\cdot 10^{-7}\ \text{cm}^{-1}.$$

This betters the results obtained by Herzberg in 1953[5] on an average of many polyads.
Again:

$$R(J) + P(J) = 2\nu_0 + (2B' - 4D') + 2(B' - B'' - 6D')J(J+1) - \\ - 2(D' - D'')J^2(J+1)^2$$

and considering that $D' \sim D''$ (where $''$ stands for the lower and $'$ for the upper state):

$$R(J) + P(J) = 2\nu_0 + 2B' + 2(B' - B'')J(J+1).$$

From the intercept and the angular coefficient of the linear fit of **Fig. 4** and by using the B value got previously:

$$B_{10^05} = (0.37453 \pm 0.00005)\ \text{cm}^{-1} \quad \text{and} \quad \nu_0 = (12774.715 \pm 0.002)\ \text{cm}^{-1}.$$

Table I. List of the observed CO_2 absorption lines. The wavenumber maximum error is 0.01 cm^{-1}.						
J	**λ at 294 K** (nm)	***R(J)*** (cm^{-1})	**σ_{max}** (10^{-26} cm^2/mol.)	**λ at 294 K** (nm)	***P(J)*** (cm^{-1})	**σ_{max}** (10^{-26} cm^2/mol.)
0	782.539	12775.47	0.1			
2	782.453	12776.88	1.3±0.3	782.682	12773.14	1.0±0.3
4	782.374	12778.16	0.6±0.3	782.787	12771.42	1.0±0.3
6	782.304	12779.31	2.3±0.2	782.901	12769.57	2.0±0.2
8	782.242	12780.33	3.6±0.2	783.022	12767.60	2.6±0.2
10	782.186	12781.24	3.5±0.2	783.150	12765.51	2.6±0.2
12	782.138	12782.02	4.6±0.1	783.286	12763.29	4.5±0.1
14	782.098	12782.67	4.8±0.1	783.430	12760.95	4.1±0.1
16	782.067	12783.19	6.1±0.1	783.581	12758.48	5.1±0.1
18	782.042	12783.60	4.8±0.1	783.740	12755.89	3.5±0.2
20	782.025	12783.87	4.9±0.1	783.908	12753.17	0.7±0.2
22	782.015	12784.03		784.082	12750.33	0.5±0.3
24	782.014	12784.05		784.265	12747.36	0.4±0.3
26	782.020	12783.95		784.455	12744.27	3.0±0.2
28	782.034	12783.73	3.5±0.2	784.653	12741.05	1.8±0.2
30	782.056	12783.37	3.1±0.2	784.859	12737.71	3.6±0.2
32	782.084	12782.90	1.9±0.2	785.072	12734.25	1.8±0.2
34	782.120	12782.31	2.0±0.2	785.294	12730.66	1.6±0.3
36	782.165	12781.58	2.1±0.2	785.523	12726.95	1.2±0.3
38	782.217	12780.74	1.3±0.3	785.760	12723.11	1.0±0.3
40	782.271	12779.77	2.3±0.2	786.004	12719.15	0.8±0.2
42	782.343	12778.67	1.1±0.3	786.257	12715.06	0.7±0.2
44	782.418	12777.45	1.1±0.3	786.517	12710.86	0.5±0.3
46	782.500	12776.11	0.1	786.785	12706.53	0.4±0.3
48	782.589	12774.65	0.1	787.061	12702.08	

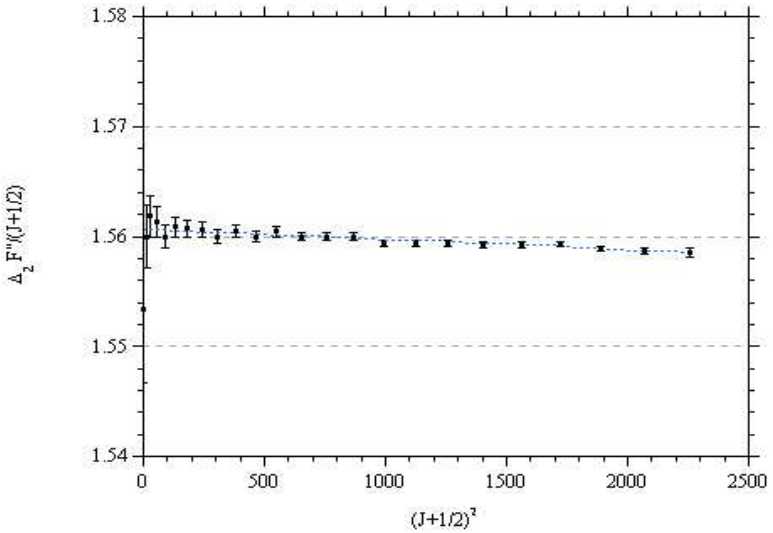

Fig. 3. Plot of $\Delta_2 F''(J)/(J + ½)$ vs $(J + ½)^2$ along with the best linear fit.

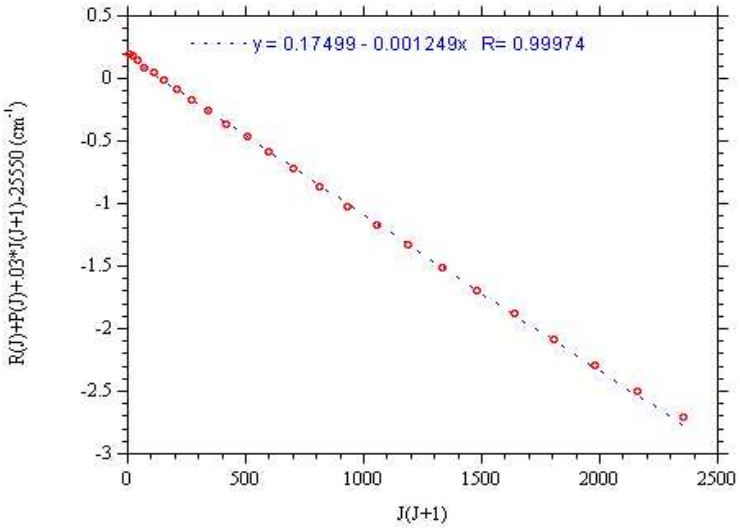

Fig. 4 Plot of $R(J)+P(J)$ vs $J(J+1)$ along with the best linear fit. The measurement errors are within the empty dots.

Methane

The methane observed absorptions belong to the combination overtone $\nu_1+3\nu_3$ [6] located at ~ 840 nm. The Roithner RLT8530G double heterostructure DL was adopted in this case as the source. The observed lines are listed in **Table II**, where preliminary results of collisional broadening and shifting coefficients are also shown for some of them.

References

[1] H. Wahlquist, *J. Chem. Phys.* **B 35** 1708 (1961); R. Arndt, *J. Appl. Phys.* **36**, 2522 (1965)
[2] S. Gerstenkorn, J. Verges, J. Chevillard, *Atlas du spectre d'absorption de la molécule d'iode*, Lab. Aimé Cotton, Orsay, Ed. CNRS (1982)
[3] B. Edlén, *Metrologia* **2**, 71 (1966)
[4] A. Campargue, D. Bailly, J.-L. Teffo, S.A. Tashkun, V.I. Perevalov, *J. Mol. Spectrosc.* **193**, 204 (1999)
[5] G. Herzberg, L. Herzberg, *J. Opt. Soc. Am.* **43**, 1037 (1953)
[6] L.P. Giver, *JQSRT* **19**, 311 (1978); J.J. O'Brien, H. Cao, *JQSRT* **75**, 323 (2002).

Table II. List of the observed CH_4 absorption lines.

Wavenum. (cm^{-1})	λ @ 21°C (Å)	σ_{max} (cm^2/molecule)	γ_{self} (MHz/Torr)	γ_{air} (MHz/Torr)	γ_{H_2} (MHz/Torr)	γ_{He} (MHz/Torr)	δ_{self} (MHz/Torr)	δ_{air} (MHz/Torr)	δ_{H_2} (MHz/Torr)	δ_{He} (MHz/Torr)
11927.40	**8381.80**	2.84E-24								
11927.00	**8382.08**									
11926.92	**8382.14**									
11926.84	**8382.19**									
11926.13	**8382.69**									
11923.17	**8384.77**	1.14E-24								
11919.23	**8387.55**	7.6E-25								
11902.20	**8399.55**	7.8E-25								
11902.08	**8399.63**									
11901.95	**8399.72**	1.19E-24								
11900.33	**8400.87**	8.0E-25								
11899.82	**8401.23**									
11898.13	**8402.42**	1.19E-24	6.1 ± 0.1	3.4 ± 0.2	4.8 ± 0.2	3.4 ± 0.2	-1.1 ± 0.1	-0.6 ± 0.1	-0.6 ± 0.1	-0.2 ± 0.1
11897.85	**8402.62**	7.4E-25	5.4 ± 0.7	3.4 ± 0.4	3.6 ± 0.5	3.0 ± 0.8	-1.4 ± 0.2	-0.9 ± 0.1	-0.7 ± 0.1	0.4 ± 0.3
11897.47	**8402.89**	8.1E-25								
11886.87	**8410.38**	1.40E-24	6.4 ± 0.1				-1.0 ± 0.1			
11886.61	**8410.56**									
11884.89	**8411.78**	2.38E-24	*Two Lines*							
11878.12	**8416.58**	4.3E-25								
11877.36	**8417.11**	1.71E-24								
11875.55	**8418.40**	7.8E-25								
11874.78	**8418.94**	7.5E-25								
11853.80	**8433.84**	1.04E-24	6.5 ± 0.1	6.2 ± 0.3	4.8 ± 0.2	3.6 ± 0.3	-0.9 ± 0.1	-0.7 ± 0.1	-0.9 ± 0.1	0.0 ± 0.1
11853.58	**8434.00**	2.5E-25								
11852.85	**8434.52**	1.30E-24								
11852.25	**8434.95**	5.3E-25								
11840.15	**8443.57**	1.71E-24	5.2 ± 0.1	3.7 ± 0.3	4.9 ± 0.2	3.2 ± 0.1	-1.5 ± 0.1	-0.9 ± 0.1	-0.8 ± 0.1	0.0 ± 0.2
11834.67	**8447.48**	3.7E-25								
11834.54	**8447.57**	1.01E-24								
11830.25	**8450.63**	1.26E-24								
11830.06	**8450.77**	5.6E-25								
11830.01	**8450.80**									
11822.33	**8456.29**	5.2E-25								
11821.99	**8456.54**	5.3E-25								
11821.79	**8456.68**	4.8E-25								
11821.67	**8456.77**									
11821.55	**8456.85**									
11821.33	**8457.01**									
11821.12	**8457.16**									
11820.83	**8457.37**	1.55E-24								
11820.67	**8457.48**	6.2E-25								
11807.44	**8466.96**	2.1E-25								